JACS
JOURNAL OF THE AMERICAN CHEMICAL SOCIETY

Article

pubs.acs.org/JACS

Mechanically Flexible Organic Crystals Achieved by Introducing Weak Interactions in Structure: Supramolecular Shape Synthons

Gamidi Rama Krishna,[‡] Ramesh Devarapalli,[‡] Garima Lal, and C. Malla Reddy*

Indian Institute of Science Education and Research (IISER) Kolkata, Mohanpur Campus, Mohanpur 741 246, India

Supporting Information

ABSTRACT: Controlling mechanical properties of ordered organic materials remains a formidable challenge, despite their great potential for high performance mechanical actuators, transistors, solar cells, photonics, and bioelectronics. Here we demonstrate a crystal engineering approach to design mechanically reconfigurable, plastically flexible single crystals (of about 10) of three unrelated types of compounds by introducing active slip planes in structures via different noninterfering supramolecular weak interactions, namely van der Waals (vdW), π-stacking, and hydrogen bonding groups. Spherical hydrophobic groups, which assemble via shape complementarity (shape synthons), reliably form low energy slip planes, thus facilitating an impressive mechanical flexibility, which allowed molding the crystals into alphabetical characters to spell out "o r g a n i c c r y s t a l". The study, which reports the preparation of a series of exotic plastic crystals by design for the first time, demonstrates the potential of soft interactions for tuning the mechanical behavior of ordered molecular materials, including those from π-conjugated systems.

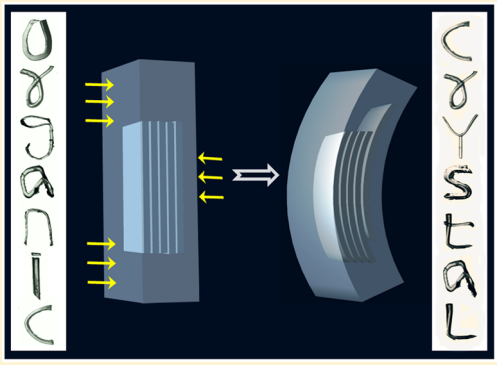

1. INTRODUCTION

Utilizing collective molecular functions from highly dense and grain boundary-free, ordered structures of organic materials is currently attractive, owing to their potential applications in mechanical actuators,[1,2] phototransistors,[3,4] light-emitting diodes (LEDs),[5] solar cells,[6] photonics,[7] integrated optical waveguides,[8] bioelectronics,[9] flexible electronics[10] etc. Although the intrinsic structure−function tunability, lightweight, and low cost advantages of the single crystalline organics over inorganic counterparts make them highly attractive, the poor mechanical performance at single particle level remains a great limitation for their practical usage on flexible substrates.[11] Ordered single crystals with high mechanical flexibility comparable to that of thin films, elastomers, and polymers can be highly advantageous for future smart materials. Although there have been increasing reports on various dynamic single crystals that, for example, show plastic or elastic flexibility,[12−14] photomechanical effect,[15−19] thermosalient effect,[20] or twisting,[21] most of these exotic single crystals are from serendipitous discoveries.

High plasticity, which is the aim of this study, can offer some unique and diverse advantages in functional molecular crystals, for instance, excellent mechanochromic luminescence (change of emission color upon mechanical action) in solid-state fluorophores,[22,23] good tabletability in API solid forms,[24,25] and lower detonation sensitivity in explosives.[26]

These recent studies have revealed excellent structural−mechanical behavior correlation, but to the best of our knowledge, not a single example was achieved by design. This goal suffers from the requirement of control over local molecular movements, which is critical in ensuring effective dissipation of stress arising from structural functions. Stress dissipation in such dynamic crystals occurs typically via the exchange or modulation of weakest intermolecular interactions, such as van der Waals (vdW), C−H···O, lighter halogens, $\pi\cdots\pi$, or a combination of these multiple forces in the structures, which is vital for preserving the monolithic nature of crystals during such macroscopic manifestations.[27]

Although the importance of the weak dispersive interactions is long acknowledged in crystal engineering[28] and materials chemistry,[29] they have been perceived as poorly dependable, and hence remained largely unexpended for accomplishing predetermined structural architectures that perform particular tasks. To overcome such a burden, here we targeted the least interfering supramolecular *shape synthons*—synthons formed via hydrophobic groups by shape complementary isotropic interactions—to rationally design mechanically flexible plastic single crystals.

2. RESULTS AND DISCUSSION

2.1. On Plastic Bending Model. Earlier hypothetical models[12,30] and recent mechanistic studies[27] on plastically bendable crystals suggest that bending proceeds by segregation of the bent section into flexible layers that slide on top of each other via reorganization of weaker intermolecular interactions (vdW and stacking), thereby generating domains with slightly different lattice orientations. Nanoindentation studies by Desiraju and Ramamurty suggest that shear sliding of the

Received: May 30, 2016
Published: July 25, 2016

DOI: 10.1021/jacs.6b05118
J. Am. Chem. Soc. 2016, 138, 13561−13567

crystallographic planes is the mechanism of plasticity in molecular crystals and it might not be necessary to invoke dislocation glide as in crystalline metals.[31,32] Hence, we targeted a structural setup with a combination of weak interactions, namely vdW (for shear sliding) and π-stacking (for splaying of molecules to accommodate the bend angle) in the perpendicular direction to achieve plastically bendable crystals.[12,27,30]

2.2. Design Strategy for Achieving Plastically Flexible Single Crystals. To move from serendipity to design, we considered the following crystal engineering strategy. A variety of noninterfering groups, namely spherical vdW groups and aromatic groups with or without hydrogen bonding functionalities (Figure 1) are strategically targeted. The near spherical

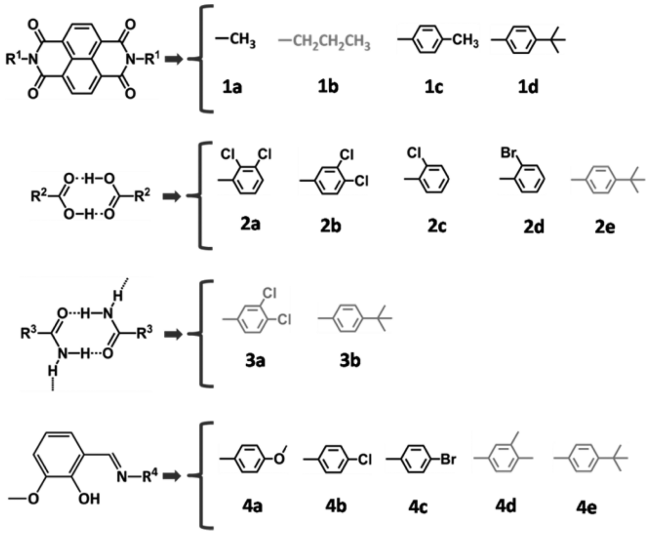

Figure 1. Building blocks utilized for achieving flexible single crystals. Derivatives that successfully resulted in flexible crystals are shown in black while those that failed are in gray.

vdW groups can potentially close pack with themselves to form smooth slip planes in the structure while the central aromatic core groups tend to close pack in the perpendicular direction, typically via π-stacking (Figure 2). In some cases, a third set of dominant hydrogen bonding groups were employed, as they also do not interfere with the above two, but prefer to form strong hydrogen bonding interactions with themselves. Here, when these hydrogen bonding groups engage themselves by forming zero dimensional (0D) homosynthons, say carboxylic acid dimers, the other two weaker type interactions shall guide the rest of the self-assembly process independently and self-sort to pack with themselves. This in turn shall lead to the formation of slip planes by vdW groups between the π-stacked columns of molecular units; a favorable condition for plastic flexibility. Notably, the vdW and π-stacking groups, both of which are weak and largely dispersive, due to the slight difference in the interaction nature and shape similarity of identical groups are expected to promote self-sorting and limit the possibility of synthon cross over, thus shall follow the proposed packing model.

To test this crystal engineering hypothesis and its general applicability, we chose three unrelated classes of molecules, (i) N-substituted naphthalene diimides (NDIs), (ii) substituted benzenes, and (iii) Schiff bases. Each class is unique and serves a different purpose: the NDI building blocks consisting of rigid covalently linked core group, represent the π-conjugated semiconducting molecular materials; the substituted benzene carboxylic acids and amides act as supramolecular building blocks where the core is uniquely constructed by hydrogen bonded acid dimer (0D) or amide (1D or 2D) synthons, hence act as prototype models for synthon based crystal engineering; Schiff bases, consisting of nonrigid unsymmetrical building blocks with a greater conformational freedom, belong to the interesting class of compounds with solid-state properties such as photochromism[33] and thermosalient nature.[34]

2.3. Covalent π-Conjugated Building Blocks: Alkyl Shape Synthons. In this series, we synthesized[35] several naphthalene diimides (NDIs), with alkyl vdW substituents such as methyl (**1a**), *n*-propyl (**1b**), *p*-tolyl (**1c**), and *tert*-butyl (**1d**) on either ends of the central NDI core, which act as covalent building blocks (Figure 1). The π-conjugated NDIs have attracted much current interest in materials science and supramolecular chemistry owing to their striking electronic (n-type semiconductors) and spectroscopic properties, and ease of preparation. The crystallization typically resulted in long needles, with lengths of up to 1 cm, and were suitable for X-ray structure determination (crystallographic information is given in SI, Table S1). Although we synthesized some halogen substituted NDI analogues, their poor solubility prevented further progress.

Analysis of crystal structures of **1a** (monoclinic $P2_1/c$), **1b** (orthorhombic *Pbca*), **1c** (monoclinic $P2_1/c$), and **1d** (triclinic *P*-1) by visual inspection revealed that in all the cases the vdW groups close pack with themselves to form the shape synthons (isotropic interactions) as anticipated while the aromatic groups form π-stacked columns in all the solids of this series. Notably in case of **1a**, **1c**, and **1d** the shape synthons align along a crystallographic plane, thus result in slip planes (except in **1b**), showing an excellent agreement with our target weak interaction based self-assemble model. For instance, in **1a** the central NDI aromatic core group forms π-stacked columns while the spherical methyl groups close pack with themselves via vdW shape synthons and form the slip planes parallel to (0 0 2) (Figure 2e). Similarly, the compounds **1c** (SI, Figure S1), **1b** and **1d** (Figure 3a) also formed the π-stacked columns separated by slip planes. Notably, in case of **1b** the elongated vdW groups (*n*-propyl) from adjacent stacks face in opposite direction.

Mechanical behavior of the crystals was examined by a simple qualitative method, i.e. applying mechanical stress using a pair of forceps and a metal needle while viewing them under a stereomicroscope.[30] To our delight, the single crystals of **1a**, **1c**, and **1d** showed excellent plastic flexibility, while notably **1b** underwent brittle fracture. The crystals of **1a**, **1c**, and **1d** could be bent to 360° (Figure 2h; videos S1, S2, and S3 corresponding to **1a**, **1c** and **1d** respectively). To demonstrate this impressive plastic flexibility, we mold the crystals of **1a** (Figure 2h) and **1d** (Figure 3b) into a variety of shapes, such as letters "S E M" and "I I R S", respectively. Such plastic flexibility is unprecedented in π-conjugated organic crystals. The bent crystals remain monolithic without much damage to the morphological integrity, even at the extreme bend angles such as in "S" and "M". All the crystals bend only on one pair of faces that is parallel to the slip plane, while they break on the perpendicular pair of faces under similar conditions (see video S4).

In the case of **1b** (brittle) the elongated $-CH_2-CH_2-CH_3$ vdW groups from stacked columns face in the opposite

DOI: 10.1021/jacs.6b05118
J. Am. Chem. Soc. 2016, 138, 13561−13567

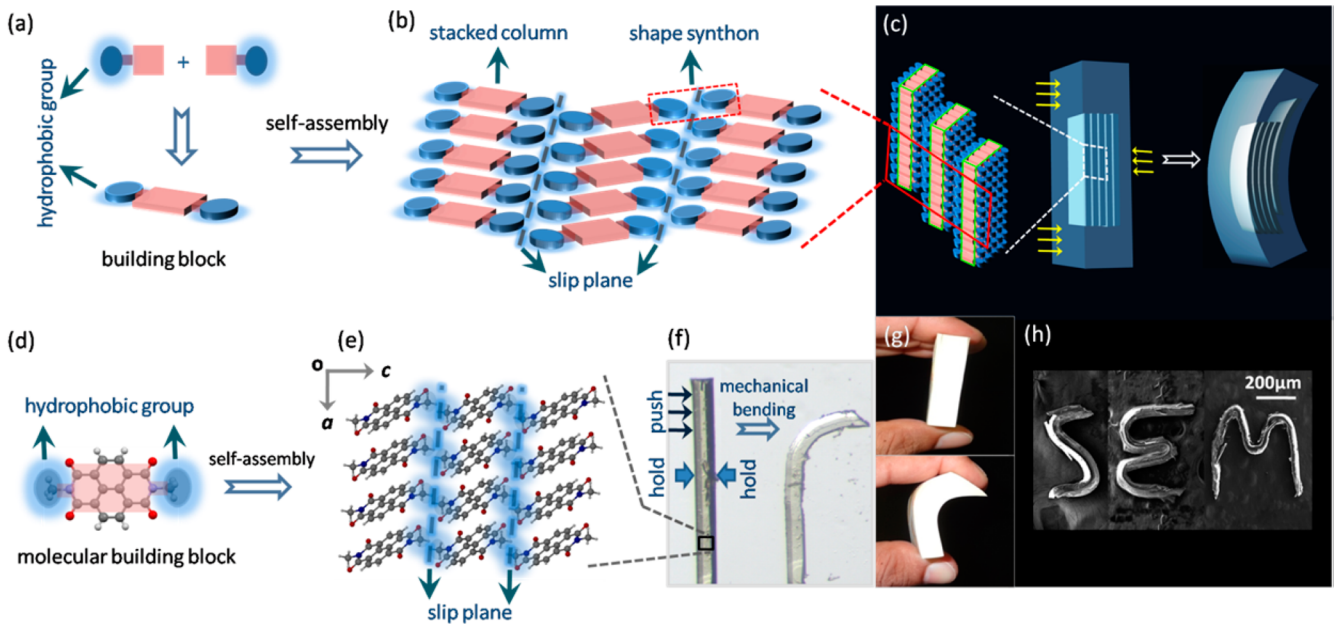

Figure 2. Illustration of the supramolecular shape synthon based, slip plane model for achieving plastic flexibility in single crystals. (a) Building block, constructed via covalent or hydrogen bonded linkages, possessing central core (in red) and peripheral vdW (in blue) groups. (b) Self-assembly of building blocks into target structural model with slip planes (broken blue lines), driven by shape synthon forming vdW groups. (c) Structural model showing the sliding of flexible molecular sheets along slip planes upon crystal bending. (d) Prototype naphthalene diimide (**1a**) based covalent building block and (e) its crystal packing, which resemble the target slip plane model in (b). (f) Micrographs of a flexible single crystal (width: 0.2 mm) of **1a**, before (left) and after (right) mechanical bending. (g) Analogy is drawn to compare the bending of a sticky yellow pad and a plastic crystal via slippage of individual sheets and slippage of molecular layers, respectively (in c and f). Notice the similarity of the top ends of the bent crystal (image on right, in f) and sticky note pad in (bottom, in g). (h) Scanning electron microscopy image of the mechanically bent crystals of **1a**.

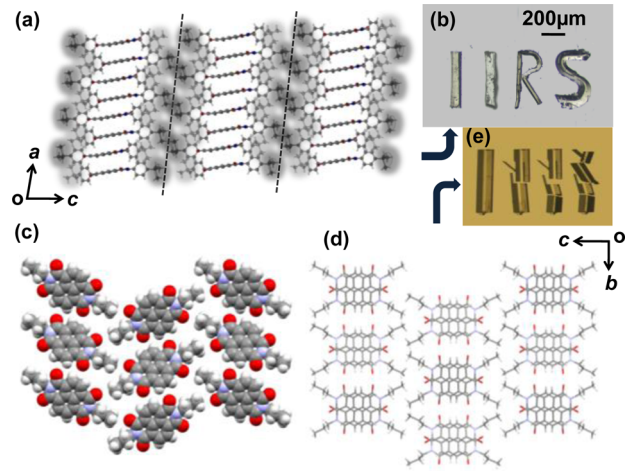

Figure 3. Crystal packing and mechanical behavior of **1b** and **1d**. (a) Crystal packing in **1d** with smooth slip planes formed by shape synthons involving spherical *tert*-butyl groups. (b) Plastic and highly flexible **1d** crystals mold into the letters "I I R S", where the first "I" corresponds to an undisturbed reference crystal and the second "I" to a crystal bent-and-reconfigured back to the original morphology. (c) Layer of **1c** molecules in the bc-plane showing a zipper type arrangement of elongated *n*-propyl groups and (d) arrangement of the next layer, where the *n*-propyl groups point in the opposite direction to that of the first and, hence, are interlocked to prevent slippage. (e) The brittle mechanical fracture of **1b** crystals.

direction, unlike in the case of spherical −Me, −*t*-Bu groups. Although the shape synthons are formed in this structure as well, the uneven surface probably prevents smooth sliding of molecular sheets and makes these crystals brittle (Figure 3c, 3d; video S4).[36] This suggests that the nearly spherical vdW groups, such as −Me and −*t*Bu, can potentially be exploited to form active slip planes, with smooth potential energy surfaces, for plastic bending.

2.4. Hydrogen Bonded Building Block: Halogen Shape Synthons. As crystal engineering strategies that work very well in one particular series may fail in another, we have extended the study to other molecules, including those with hydrogen bonding groups. The molecular units employed in this series possess a carboxylic acid or amide group. The supramolecular dimer formed by these groups acts as a central core, in place of the rigid covalent moiety in the NDI series (Figure 1). The vdW groups here are mostly halogen groups (Cl, Br), except in **2e** (−*t*-Bu), which are substituted on the aromatic ring. The lighter halogens are expected to form soft halogen···halogen (X···X) interactions.[37−39] Halogen interactions are generally classified into two categories: type I (geometrical) and type II (chemical, polarization based). The type I X···X interactions, which are more favored by the lighter halogens Cl and Br, are nonpolar and typically interact based on shape complementarity; hence, they qualify as shape synthons (softer type) desired for our model. On the contrary, the heaviest halogen group, iodine, prefers the polarization based stronger type II X···X interactions (harder type) and,[37] hence, is not desirable.

The dichloro compounds, **2a** ($C2/c$) and **2b** ($P2_1/c$), form the carboxylic acid dimers (0D) via cyclic O−H···O hydrogen bonds (Table S2, Hydrogen bond table). These dimers further pack into columns along the *b*-axis with only π-stacking interactions. As anticipated, the Cl groups in both **2a** and **2b** not only form type I Cl···Cl (in **2a**: 3.486 Å, 159.79°, 124.83°; in **2b**: 3.492 Å, 172.34°, 116.70°) shape synthons, but also aligned to form slip planes parallel to (0 0 1) in both cases. This is very significant, as despite the different geometrical

DOI: 10.1021/jacs.6b05118
J. Am. Chem. Soc. 2016, 138, 13561−13567

positioning of Cl groups in **2a** (2,3-) and **2b** (3,4-), they form the slip planes in a similar manner, demonstrating the driving potential of Cl groups for forming the shape synthons. Not only this, the crystals of both **2a** and **2b** showed high plastic bending flexibility upon mechanical action, demonstrating the striking agreement with the proposed model.

The monohalo-compounds, **2c** (2-chlorobenzoic acid) and **2d** (2-bromobenzoic acid), also form dimers that pack into columns in the structure. The slip planes are also formed in them, but are not entirely by the halogen groups. The single halogen group (less surface area, compared to the dihalo-compounds) and the edge-to-edge aromatic interactions (which are also vdW type) (SI, Figure S2) contribute to the slip plane. These two crystals also show plastic flexibility, which is demonstrated by shaping them into the letters "o r g a n i c c r y s t a l" (Figure 4c). While the simple

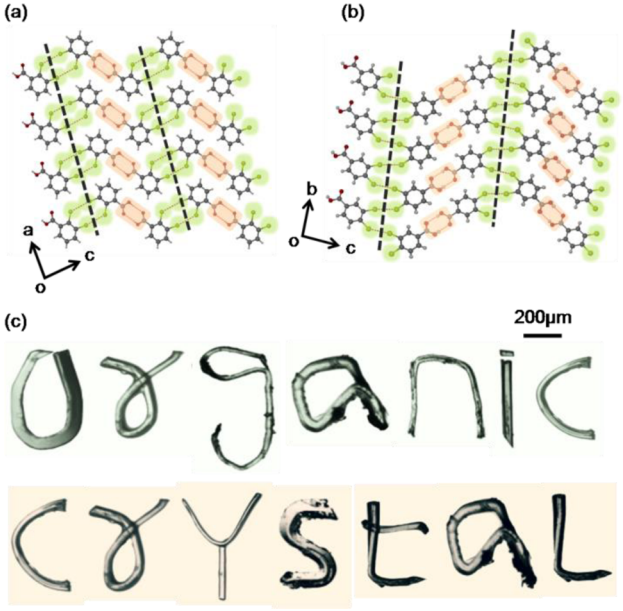

Figure 4. Halogen shaped synthons on supramolecular building blocks: Crystal letters: Crystal packing in (a) 2,3-dichlorobenzoic acid, **2a**, and (b) 3,4-dichlorobenzoic acid, **2b**, to show the formation of shape synthons by Cl-groups (in green) and 0D acid dimers (in red). Flexible crystals of (c) **2a**, **2b**, **2c**, and **2d** modulated into the letters "o r g a n i c c r y s t a l".

benzoic acid fails to show plastic flexibility, perhaps due to the absence of any soft vdW groups and the presence of more specific C−H···O interactions between slip stacked molecules in the structure (SI, Figure S3).

To test if the presence of slip planes in crystals alone is sufficient or if the absence of extended hydrogen bonds is also needed for plastic flexibility, some primary amide analogues were also studied. Because, in contrast to the 0D acid dimers, amides typically form extended 1D chains or 2D sheets due to the presence of additional N−H group. We succeeded to synthesize and obtain suitable single crystals of amides, **3a** (3,4-dichlorobenzamide) and **3b** (*p*-tertiarybutyl benzamide, see Figure 1). Remarkably, in both **3a** and **3b** the vdW groups again close pack with themselves across a plane in the crystals to form the desired slip planes (Figure 5). However, both the crystals were found to be brittle and showed no sign of plastic flexibility.

This suggests that the presence of strong N−H···O interactions in 1D and 2D networks may make the structure rigid, hence can prevent local molecular movements in crystals (Figure 5). Moving entire sheet or layer at a time for mechanical shearing is energetically expensive, i.e. the shear stress becomes greater than fracture stress. Hence the hydrogen bonded sheets may act as *rigid sheets* rather than *flexible sheets*. This suggests that in addition to the "softness" of the X···X or R···R interactions, the absence of *rigid* extended interactions in the structure is critical in providing such malleability to crystals. Stronger, but also "harder" interactions such as hydrogen bonding as seen in **3a** and **3b** would accumulate larger stress at short distances, and contribute to enhanced stiffness to cause fracture of the crystal.

2.5. Unsymmetrical Building Blocks with Multiple Types of vdW Groups. Contrary to the symmetrical building blocks in the two earlier categories, in this series there are some unsymmetrical Schiff bases of a pharmaceutically significant *o*-vanillin compound, with greater conformational flexibility and multiple types of vdW groups. All the building blocks in this series, which are easy to prepare, have a common − OMe group (from vanillin) on one end and − OMe, − Cl, −Br, −Me, or −*t*-Bu on the opposite end (from substituted anilines), while the central part consists of −C═N− (Figure 1). Hence, this increased complexity (unsymmetrical molecular geometry with different functional groups on two ends and greater conformational flexibility) provides a good test for assessing the reliability and generality of our proposed design model.

Analysis of crystal structures revealed that majority of the structures are indeed consistent with the proposed model (Figure 6(a) and 6(b)). For instance, in **4a** the slip planes are formed by the two − OMe groups on either ends (SI, Figure S6) while the aromatic groups form the π-stacking interactions in the orthogonal direction, which result in a corrugated packing. The compounds **4b** and **4c**, which are isostructural ($P2_12_12_1$), also form slip planes by close packing of − OMe, − Cl/−Br and aromatic C−H groups (Figure 6(a) and 6(b)). On the other hand, compounds, **4d** and **4e**, with purely alkyl substituents (−Me, −*t*-Bu groups, respectively, on the aniline side) failed to form slip planes, unlike in the successful cases of **1a** and **1d** with the same groups, respectively. The qualitative mechanical tests revealed that the crystals of **4a** to **4c** are highly flexible and bend plastically, while **4d** and **4e** did not show plastic flexibility under similar conditions. In the latter two crystals, the crystal structures adopt the π-stacked layer arrangement with no slip planes by the vdW groups.[12] The failure of vdW groups to form slip planes in this complex system can be attributed to the interference from electronegative groups (formation of sp^3C−H···O between −OMe groups) on these molecules (SI, Figures S7 and S8). Nevertheless, the model has facilitated a fair success even in this complex series.

2.6. Calculated Attachment Energies: Identification of Low Energy Active Slip Planes. The attachment energy, E_{att}, is the energy released upon attachment of a growth slice to the growing face of a crystal. The $E_{att} = E_{latt} - E_{slice}$, where E_{latt} is the lattice energy, and E_{slice} is the energy released on the attachment of a growth slice of a thickness equal to the interplanar *d*-spacing for the crystallographic plane representing the face. Calculated E_{att} data of all the crystals in this study (SI, Table S3) show an excellent agreement with the slip planes identified by visual inspection of respective crystal structures. Notably, in all the plastic bending crystals, the slip planes formed by the specifically chosen vdW groups for this model always possess the lowest E_{att}, as evident from the listed E_{att}

DOI: 10.1021/jacs.6b05118
J. Am. Chem. Soc. 2016, 138, 13561−13567

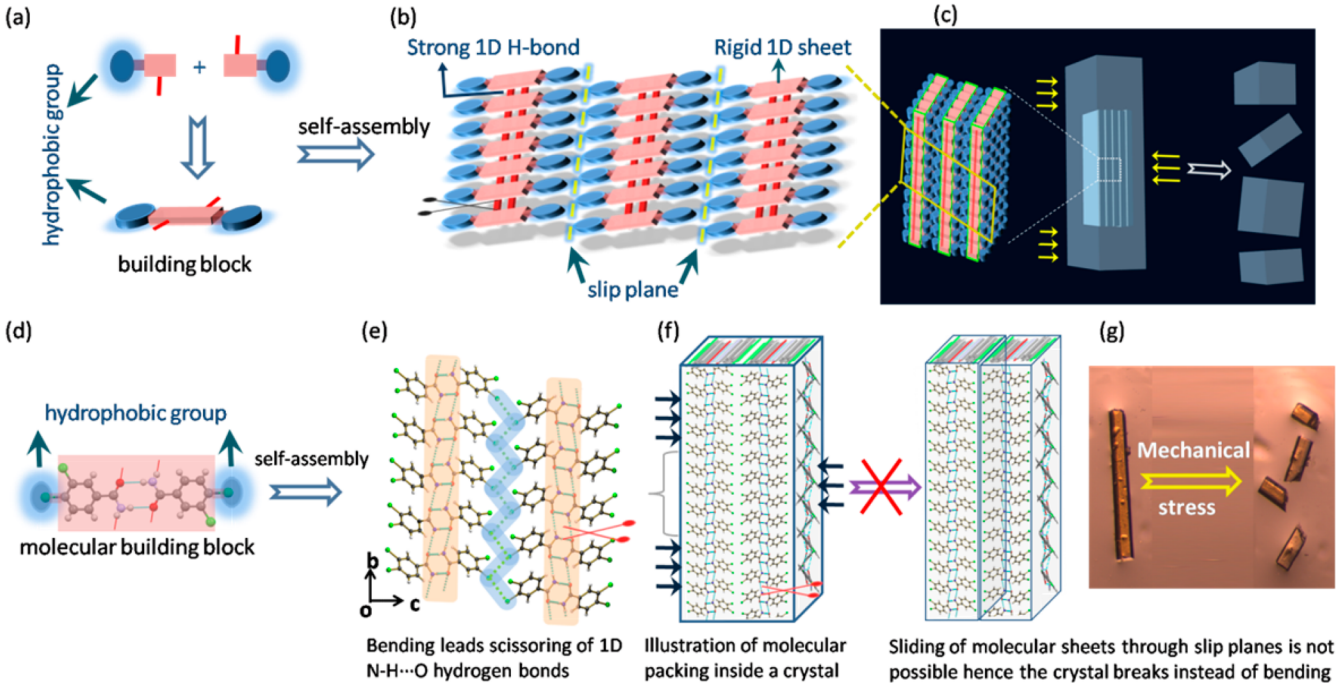

Figure 5. Schematic representation of brittle fracture in amides. (a) Formation of building block and (b) packing of molecules into hydrogen bonded sheets, separated by slip planes. The strong extended H-bonds make the sheets rigid. (c) Tight packing of molecules within the rigid sheet prevents splaying of molecules; hence, fracture ensues. (d) Amide based molecular building block. (e) Formation of 1D N−H···O hydrogen bonds and supramolecular shape synthons via Cl···Cl interactions. (f) Illustration of the molecular packing with 1D hydrogen bonded sheets separated by slip planes in the crystal. Sliding of layers requires the movement of an entire sheet at a time due to its rigidity; splaying of molecules is also restricted by extended hydrogen bonding, thus the crystals break instead of plastic bending. (g) Fracture of crystals of **3a** upon application of a mechanical stress.

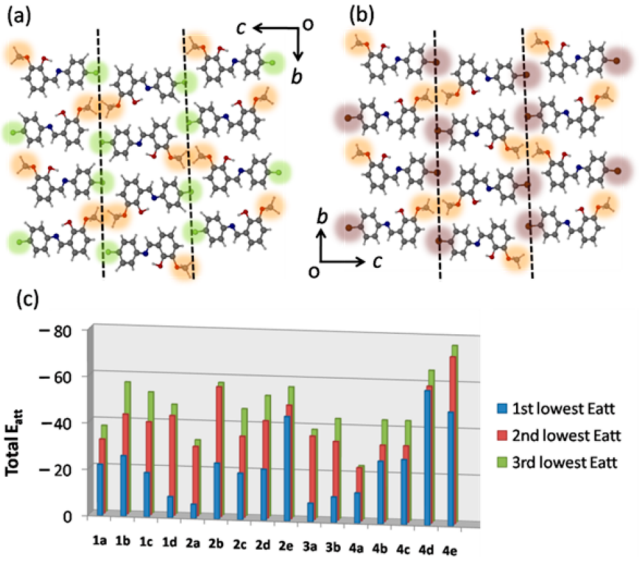

Figure 6. Formation of shape synthons in unsymmetrical Schiff base building blocks. (a) Packing in (E)-2-((4-chlorophenylimino)methyl)-6-methoxyphenol, **4b**, and (b) (E)-2-((4-bromophenylimino)methyl)-6-methoxyphenol, **4c**, shows the formation of slip planes by multiple vdW groups, −OMe (yellow) and Cl (green)/Br (gray). (c) Plot shows the first three lowest attachment energies of all the studied molecules. In all the cases, the first lowest E_{att} shows a good agreement with the visually identified slip plane.

values of the three weakest planes of each structure, shown in Figure 6c (also see SI, Table S3). Hence, this not only justifies the choice of our vdW groups, but also their reliable transferability to other molecules.

The fair success of the model in the three above classes of molecules demonstrates the potential of weaker interactions for reliably achieving desired structures, which we feel is important in the context of crystal engineering. The successful examples of ten plastically flexible crystals from the three different types of compounds demonstrate that the proposed model has potential to be transferred to other functional materials, while the failed cases provided further insights into the structural requirement for plastic flexibility. The study may act as a good starting point to further improvise the strategies to design future stimuli responsive dynamic crystalline materials.

3. CONCLUSIONS

Here we successfully demonstrated a crystal engineering strategy to achieve plastically flexible single crystals by introducing active slip planes in the structure by carefully placing selected noninterfering van der Waals (such as −*t*-Bu, −OMe, −Me, −Cl/Br, etc.), π-stacking, and hydrogen bonding groups, on three different classes of compounds. The key factor for achieving the desired crystal packing with low frictional planes, as required by the bending model, is primarily the noninterfering and self-sorting nature of the selected functional groups, i.e. (i) the van der Waals (vdW) groups, (ii) hydrogen bonding groups that form 0D cyclic hydrogen bonded dimers, and (iii) the aromatic π-stacking groups. The dispersive nature of the vdW groups with spherical shape has favored formation of smooth molecular planes with least attachment energy (i.e., active slip planes) in the structure. The vdW shape synthons act as lubricated planes and allow molecular motions with minimal friction between molecular sheets. These groups allow sliding of molecules upon mechanical action while the π-stacking interactions aid the flexibility of sheets during mechanical

DOI: 10.1021/jacs.6b05118
J. Am. Chem. Soc. 2016, 138, 13561−13567

bending. The absence of extended *rigid* hydrogen bonding networks is also a key factor for facilitating plastic flexibility in crystals. It appears that the strong self-sorting and non-interfering nature of the three distinct types of groups employed here is not only important for driving crystal packing, but also probably critical for preserving the short-range structural order and promoting coordinated molecular movements in the process of crystal bending. The three diverse series studied here emphasize the potential of various weak vdW interactions for achieving plastic flexibility. Further, these unexploited weak interactions can also allow tuning the properties of diverse types of stimuli responsive organic solids. The well coordinated local molecular movements involved here are comparable to the supramolecular structural changes that generally occur in many other dynamic crystalline materials. Hence, our first design approach potentially has broad implications for materials chemistry. Quantification of the mechanical properties by the nanoindentation technique on the number of crystals studied here is planned for the future.

4. EXPERIMENTAL SECTION

4.1. Materials. All the reagents were purchased from Sigma-Aldrich. Commercially available solvents were used (for synthesis and crystallization) as received without further purification.

4.2. Synthesis. *4.2.1. NDI Derivatives.* N,N′-Bis(methyl)-1,4,5,8-naphthalene diimide (**1a**), N,N′-bis(*n*-propyl)-1,4,5,8-naphthalene diimide (**1b**), N,N′-bis(*p*-tolyl)-1,4,5,8-naphthalene diimide (**1c**), and N,N′-bis(*p*-tertiarybutylphenyl)-1,4,5,8-naphthalene diimide (**1d**) were synthesized by condensation of the carboxylic acid dianhydride with two equivalents of the respective substituted amines in DMF at temperatures above 110 °C for overnight.[35] All the obtained compounds were purified by recrystallization and characterized by using ^{1}H NMR and X-ray structure determination.

4.2.2. Amides. 3,4-Dichloro benzamide (**3a**) and 4-tertiarybutyl benzamide (**3b**) were prepared from previously reported procedure.[40]

4.2.3. Imines. All five imines **4a**, **4b**, **4c**, **4d**, and **4e** were prepared by solid state mechanical grinding of *o*-vanillin and respective substituted aniline taken in 1:1 stoichiometric ratio.[41]

4.3. Preparation of Single Crystals. The derivatives of all NDIs were recrystallized from dichloromethane and all remaining compounds were recrystallized from diethyl ether by slow evaporation at ambient conditions. Crystals suitable for testing mechanical properties and single crystal data were obtained in 4 to 5 days in all the cases.

4.4. Single Crystal X-ray Structure Determination. Single crystals of all the compounds were individually mounted on a glass pip. Intensity data of all the compounds (except **2e**, **3b**, and **4e**) were collected on a Bruker's KAPPA APEX II CCD Duo system with graphite-monochromatic Mo Kα radiation (λ = 0.71073 Å). The data for **1a**, **1c**, and **3b** were collected at 100 K and all other compounds were collected at 296 K. Data reduction was performed using Bruker SAINT software.[42] Crystal structures were solved by direct methods using SHELXL-97 and refined by full-matrix least-squares on F^2 with anisotropic displacement parameters for non-H atoms using SHELXL-97.[43] Hydrogen atoms associated with carbon atoms were fixed in geometrically constrained positions. Hydrogen atoms associated with oxygen and nitrogen atoms were included in the located positions. Structure graphics shown in the figures were created using the X-Seed software package version 2.0.[44]

Intensity data of **2e**, **3b**, and **4e** single crystals were collected on a Oxford Diffraction SuperNova (Dual, Eos) diffractometer with monochromatic Mo-Kα radiation (λ = 0.71073 Å). The crystals of **2e** and **3b** were measured at 100 K and **4e** at 296 K. The data reduction was done with *CrysAlis PRO and* structures were solved using Olex2,[45] with the Superflip[46] structure solution program using Charge Flipping and refined with the ShelXL[47] refinement package using Least Squares minimization.

4.5. Scanning Electron Microscopy (SEM). High resolution SEM was performed on a Zeiss microscope; SUPRA 55VP-Field Emission Scanning Electron Microscope. High performance variable pressure FE-SEM with patented GEMINI column technology. Schottky 5 type field emitter system, single condenser with crossover-free beam path. Resolution: 1.0 nm at 15 kV; 1.6 nm at 1 kV high vacuum mode. 2.0 nm at 30 kV at variable pressure mode.

4.6. Attachment Energies. The attachment energies of all the crystals were computed by Crystal Graph software using Dreiding force field and Gesteiger charges. The attachment energies were computed at medium quality using inputs from Crystal Graph.

■ ASSOCIATED CONTENT

Supporting Information

The Supporting Information is available free of charge on the ACS Publications website at DOI: 10.1021/jacs.6b05118.

^{1}H NMR data, crystal packing diagrams with respective crystal images depicting mechanical deformation, tables containing crystallographic information and geometrical parameters of hydrogen bonding, ORTEP diagrams, and a table of attachment energy values for each compound (PDF)

Video of bending of crystals of **1a** (MPG)

Video of bending of crystals of **1c** (MPG)

Video of bending of crystals of **1d** (MPG)

Video showing breaking on the perpendicular pair of faces (MPG)

CIF data for N,N'-bis(methyl)-1,4,5,8-naphthalene diimide (CIF)

CIF data for N,N′-bis(*n*-propyl)-1,4,5,8-naphthalene diimide (CIF)

CIF data for N,N-bis(*p*-tolyl)-1,4,5,8-naphthalene diimide (CIF)

CIF data for N,N′-bis(*p*-tertiarybutylphenyl)-1,4,5,8-naphthalene diimide (CIF)

CIF data for 2,3-dichloro benzoic acid (CIF)

CIF data for 3,4-dichloro benzoic acid (CIF)

CIF data for 2-chloro benzoic acid (CIF)

CIF data for 2-bromo benzoic acid (CIF)

CIF data for 3,4-dichloro benzamide (CIF)

CIF data for 4-tertiarybutyl benzamide (CIF)

CIF data for *o*-vanilidene *p*-methoxyaniline (CIF)

CIF data for *o*-vanilidene 3,4-dimethylaniline (CIF)

CIF data for *o*-vanilidene *p*-tertiarybutylaniline (CIF)

■ AUTHOR INFORMATION

Corresponding Author

*cmreddy@iiserkol.ac.in or cmallareddy@gmail.com

Author Contributions

‡G.R.K. and R.D. contributed equally.

Notes

The authors declare no competing financial interest.

■ ACKNOWLEDGMENTS

C.M.R. acknowledges financial support from the CSIR (02(0156)/13/EMR-II). G.R.K., R.D., and G.L. thank IISER-Kolkata for a fellowship. The authors thank Dr. Tejender S. Thakur (CSIR-Central Drug Research Institute, Lucknow, India), for the attachment energy calculations.

■ REFERENCES

(1) Zhang, Q. M.; Li, H.; Poh, M.; Xia, F.; Cheng, Z. Y.; Xu, H.; Huang, C. *Nature* **2002**, *419*, 284.

DOI: 10.1021/jacs.6b05118
J. Am. Chem. Soc. 2016, 138, 13561−13567

(2) Yao, Z. S.; Mito, M.; Kamachi, T.; Shiota, Y.; Yoshizawa, K.; Azuma, N.; Miyazaki, Y.; Takahashi, K.; Zhang, K.; Nakanishi, T.; Kang, S.; Kanegawa, S.; Sato, O. *Nat. Chem.* **2014**, *6*, 1079.
(3) Briseno, A. L.; Tseng, R. J.; Ling, M. M.; Falcao, E. H. L.; Yang, Y.; Wudl, F.; Bao, Z. *Adv. Mater.* **2006**, *18*, 2320.
(4) Tang, B. Q.; Li, L.; Song, Y.; Liu, Y.; Li, H.; Xu, W.; Liu, Y.; Hu, W.; Zhu, D. *Adv. Mater.* **2007**, *19*, 2624.
(5) Ou, E. C.W.; Hu, L.; Raymond, G. C. R.; Soo, O. K.; Pan, J.; Zheng, Z.; Park, Y.; Hecht, D.; Irvin, G.; Drzaic, P.; Gruner, G. *ACS Nano* **2009**, *3*, 2258.
(6) Günes, S.; Neugebauer, H.; Sariciftci, N. S. *Chem. Rev.* **2007**, *107*, 1324.
(7) Dalton, L. R.; Harper, A. W.; Ghosn, R.; Steier, W. H.; Ziari, M.; Fetterman, H.; Shi, Y.; Mustacich, R. V.; Jen, A. K. Y.; Shea, K. J. *Chem. Mater.* **1995**, *7*, 1060.
(8) Chandrasekhar, N.; Chandrasekar, R. *Angew. Chem., Int. Ed.* **2012**, *51*, 3556.
(9) Wu, W.; Wen, X.; Wang, Z. L. *Science* **2013**, *340*, 952.
(10) Rogers, J. A.; Someya, T.; Huang, Y. *Science* **2010**, *327*, 1603.
(11) Varughese, S.; Kiran, M. S. R. N.; Ramamurty, U.; Desiraju, G. R. *Angew. Chem., Int. Ed.* **2013**, *52*, 2701.
(12) Reddy, C. M.; Padmanabhan, K. A.; Desiraju, G. R. *Cryst. Growth Des.* **2006**, *6*, 2720.
(13) Ghosh, S.; Reddy, C. M. *Angew. Chem., Int. Ed.* **2012**, *51*, 10319.
(14) Takamizawa, S.; Takasaki, Y. *Angew. Chem., Int. Ed.* **2015**, *54*, 4815.
(15) Morimoto, M.; Irie, M. A. *J. Am. Chem. Soc.* **2010**, *132*, 14172.
(16) Naumov, P.; Chizhik, S.; Panda, M. K.; Nath, N. K.; Boldyreva, E. *Chem. Rev.* **2015**, *115*, 12440.
(17) Kim, T.; Al-Muhanna, M. K.; Al-Suwaidan, S. D.; Al-Kaysi, R. O.; Bardeen, C. J. *Angew. Chem., Int. Ed.* **2013**, *52*, 6889.
(18) Zhu, L.; Al-Kaysi, R. O.; Bardeen, C. J. *J. Am. Chem. Soc.* **2011**, *133*, 12569.
(19) Medishetty, R.; Sahoo, S. C.; Mulijanto, C. E.; Naumov, P.; Vittal, J. J. *Chem. Mater.* **2015**, *27*, 1821.
(20) Sahoo, S. C.; Sinha, S. B.; Kiran, M. S. R. N.; Ramamurty, U.; Dericioglu, A. F.; Reddy, C. M.; Naumov, P. *J. Am. Chem. Soc.* **2013**, *135*, 13843.
(21) Shtukenberg, A. G.; Punin, Y. O.; Gujral, A.; Kahr, B. *Angew. Chem., Int. Ed.* **2014**, *53*, 672.
(22) Krishna, G. R.; Kiran, M. S. R. N.; Fraser, C. L.; Ramamurty, U.; Reddy, C. M. *Adv. Funct. Mater.* **2013**, *23*, 1422.
(23) Krishna, G. R.; Devarapalli, R.; Prusty, R.; Liu, T.; Fraser, C. L.; Ramamurty, U.; Reddy, C. M. *IUCrJ* **2015**, *2*, 611.
(24) Krishna, G. R.; Shi, L.; Bag, P. P.; Sun, C. C.; Reddy, C. M. *Cryst. Growth Des.* **2015**, *15*, 1827.
(25) Bag, P. P.; Chen, M.; Sun, C. C.; Reddy, C. M. *CrystEngComm* **2012**, *14*, 3865.
(26) Zhang, C.; Wang, X.; Huang, X. *J. Am. Chem. Soc.* **2008**, *130*, 8359.
(27) Panda, M. K.; Ghosh, S.; Yasuda, N.; Moriwaki, T.; Mukherjee, G. D.; Reddy, C. M.; Naumov, P. *Nat. Chem.* **2015**, *7*, 65.
(28) Desiraju, G. R.; Steiner, T. *The Weak Hydrogen Bond in Structural Chemistry and Biology*; Oxford University Press: Oxford, 1999.
(29) Azuri, I.; Adler-Abramovich, L.; Gazit, E.; Hod, O.; Kronik, L. *J. Am. Chem. Soc.* **2014**, *136*, 963.
(30) Reddy, C. M.; Krishna, G. R.; Ghosh, S. *CrystEngComm* **2010**, *12*, 2296.
(31) Raut, D.; Kiran, M. S. R. N.; Mishra, M. K.; Asiri, A. M.; Ramamurty, U. *CrystEngComm* **2016**, *18*, 3551.
(32) Kiran, M. S. R. N.; Varughese, S.; Reddy, C. M.; Ramamurthy, U.; Desiraju, G. R. *Cryst. Growth Des.* **2010**, *10*, 4650.
(33) Hadjoudis, E.; Mavridis, I. M. *Chem. Soc. Rev.* **2004**, *33*, 579.
(34) Ghosh, S.; Mishra, M. K.; Ganguly, S.; Desiraju, G. R. *J. Am. Chem. Soc.* **2015**, *137*, 9912.
(35) Molla, M. R.; Das, A.; Ghosh, S. *Chem. - Eur. J.* **2010**, *16*, 10084.
(36) Efforts are currently underway to study this case by computational techniques.
(37) Reddy, C. M.; Kirchner, M. T.; Gundakaram, R. C.; Padmanabhan, K. A.; Desiraju, G. R. *Chem. - Eur. J.* **2006**, *12*, 2222.
(38) Priimagi, A.; Cavallo, G.; Metrangolo, P.; Resnati, G. *Acc. Chem. Res.* **2013**, *46*, 2686.
(39) Mukherjee, A.; Tothadi, S.; Desiraju, G. R. *Acc. Chem. Res.* **2014**, *47*, 2514.
(40) Heilman, P. W.; Battershell, R. D.; Pyne, W. J.; Goble, P. H.; Magee, T. A.; Matthews, R. J. *J. Med. Chem.* **1978**, *21*, 906.
(41) Correia, I.; Pessoa, J. C.; Duarte, M. T.; Piedade, M. F. M.; Jackush, T.; Kiss, T.; Margarida, M.; Castro, C. A.; Geraldes, C. F. G. C.; Avecilla, F. *Eur. J. Inorg. Chem.* **2005**, *2005*, 732.
(42) *SAINT Plus* (version 6.45); Bruker AXS Inc.: Madison, WI, 2003.
(43) *SMART* (version 5.625) and SHELX-TL (version 6.12); Bruker AXS Inc.: Madison, WI, 2000.
(44) Barbour, L. J. *X-Seed—Graphical Interface to SHELX-97 and POV-Ray*; University of Missouri, Columbia: Columbia, MO, USA, 1999.
(45) Dolomanov, O. V.; Bourhis, L. J.; Gildea, R. J.; Howard, J. A. K.; Puschmann, H. *J. Appl. Crystallogr.* **2009**, *42*, 339.
(46) Palatinus, L.; Chapuis, G. *J. Appl. Crystallogr.* **2007**, *40*, 786.
(47) Sheldrick, G. M. *Acta Crystallogr., Sect. A: Found. Crystallogr.* **2008**, *64*, 112.

DOI: 10.1021/jacs.6b05118
J. Am. Chem. Soc. 2016, 138, 13561−13567